# P2.8 COMBINATION OF MEASUREMENTS FROM A MILLIMETER WAVE CLOUD RADAR AND A HIGH SPECTRAL RESOLUTION LIDAR AT EUREKA

Jasmine Rémillard* and Pavlos Kollias
McGill University, Montréal, Québec, Canada

Edwin W. Eloranta
University of Wisconsin-Madison, Madison, Wisconsin

Matthew D. Shupe
CIRES, University of Colorado and NOAA ESRL, Boulder, Colorado

## 1 INTRODUCTION

Clouds play a critical role in Earth's climate through the reflection, absorption and emission of radiation, the vertical transport of heat and moisture and the generation of precipitation and its associated latent heat release and evaporation. Despite ever increasing computational power and model sophistication, the poor representation of cloud processes continues to be one of the major sources of uncertainty in numerical simulations of climate and weather.

Climatologies of cloud occurrence (cloud fraction), vertical extend and altitude, hydrometeor size and phase are required in order to assess the current effect of clouds on Earth's climate and to help predict their future contribution to Earth's radiation budget. Millimeter-wavelength radars (radars sensitive to small cloud droplets or cloud radars) and lidars are capable of resolving with good accuracy the vertical distribution of cloud layers and can be used to produce cloud type climatology with vertical layering information. In addition to cloud layering (e.g., Clothiaux et al., 2000), synergetic measurements from cloud radars and lidars have been used in the past to infer hydrometeor type and phase (e.g., Shupe, 2007; Shupe et al., 2006).

The life cycles and radiative properties of clouds are highly sensitive to the phase of their hydrometeors (i.e., liquid or ice). Knowledge of cloud phase is essential for specifying the optical properties of clouds, or else, large errors can be introduced in the calculation of cloud radiative fluxes (e.g., Gregory and Morris, 1996). This is particularly true at high latitudes where subzero temperatures persist most of the year in the temperature range from 0 to $-40$°C, where both liquid and ice hydrometeor phases (mixed-phase) are sustainable (Shupe et al., 2006).

The US Department of Energy Atmospheric Radiation Measurement (ARM) program (Ackerman and Stokes, 2003) operates several cloud-radiation observations at ground-based sites around the globe (www.arm.gov), providing long records of detailed measurements of clouds from an array of active and passive remote sensors. In addition, the Canadian Network for the Detection of Atmospheric Changes (CANDAC) operates a similar ground-based facility at Eureka, near the Arctic Circle, and NASA's recently launched CloudSat/CALIPSO satellites, that carry the first spaceborne cloud radar and lidar for cloud-precipitation-aerosol measurements, offer additional measurements of clouds. Here, we use examples of observations from the Canadian site at Eureka to demonstrate the potential of retrieving cloud occurrence, type and phase. Future plans call for an extensive network of atmospheric observations circling the Arctic to provide the state of this polar atmosphere and its clouds.

## 2 OBSERVATIONS

Synergetic, ground-based measurements from a combination of active remote sensors is a very popular observational approach to study cloud properties. Eureka is the highest northern latitude cloud and radiation observatory: its coordinates are 79°59′25″N, 85°56′20″W, which put it on the Ellesmere Island, very close to the Arctic Circle

*Corresponding author address: Jasmine Rémillard, McGill University, Dept. of Atmospheric and Oceanic Sciences, Montréal, QC; e-mail: jasmine.remillard@mail.mcgill.ca

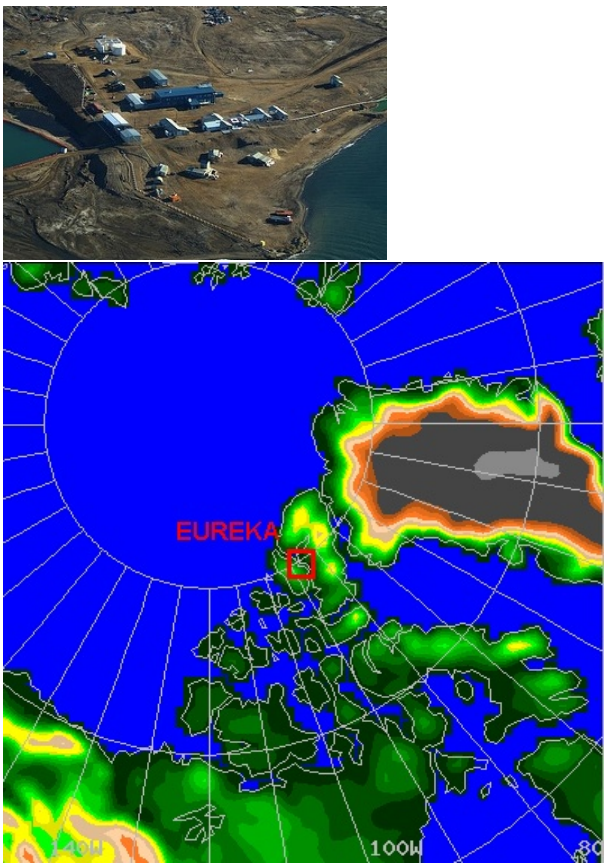


Figure 1: Location of Eureka and its facilities.

(see Fig. 1). Among the instruments already in place in Eureka are an atmospheric emitted radiation interferometer (AERI), a millimeter wave cloud radar (MMCR, Moran et al., 1998), a high spectral resolution lidar (HSRL, Eloranta, 2005) and a microwave radiometer. There is also a weather station and soundings of the atmosphere are taken every 12 hours. More than 15 months of coincident MMCR and HSRL measurements are used in this study. A summary of the main technical characteristics of the active remote sensors appears in table 1, while a more detailed description follows.

Eureka is unique not only for its high latitude location, but also because it is the only cloud-radiation observatory where this combination (MMCR/HSRL) of high-performance cloud instruments is found. Thus, a thorough analysis of the measurements is encouraged. The co-location of the MMCR and HSRL in a same seatainer (see Fig. 2) facilitates greatly the combination of their data: they are basically looking at the same atmospheric column. Moreover, they started operating on an automated, continuous manner at Eureka the same day, August

Figure 2: The MMCR and HSRL in their seatainer, near Eureka. The former is visible from its antenna on the top of the light blue seatainer, while the latter is recognized by its window, behind the MMCR antenna.

12, 2005.

### 2.1 MMCR

The MMCR is a vertically pointing, unattended, Doppler cloud radar. It is identical to the MMCR operated by the ARM program and, as its name indicates, it works in the millimeter wavelength region of the electromagnetic spectra, more precisely at 8.66 mm, which corresponds to a frequency of 34.86 GHz. The MMCR cycles through four operating modes, each having its own utility (Clothiaux et al., 2000). Its high radar sensitivity is possible due to its high duty cycle, large antenna, long time samples and pulse compression techniques (Moran et al., 1998). The data collected from each mode are merged together to give the resolutions given in table 1. Although the MMCR measures the full Doppler spectra at each gate, only the Doppler moments (reflectivity factor, Doppler velocity and spectral width) are used in this study.

### 2.2 HSRL

The HSRL is operated by Ed Eloranta's research group at the University of Wisconsin. It is an unattended vertically pointing lidar. It uses the line 309 of the iodine spectrum, which is in the green range. The HSRL resolution indicated in table 1 are the maximal attainable. The data are usually averaged to coarser resolution in order to reduce the noise. For instance, the data used in this project have resolutions of 30 m and 180 s.

The glass window allowing the HSRL signal to get into the atmosphere and back is sloped and heated, to prevent any snow or water accumulation on it,

| | MMCR | HSRL |
|---|---|---|
| Wavelength | 8.66 mm (34.86 GHz) | 532 nm |
| Average power | 25 W | 0.6 W |
| Beam width | 0.3°, circular | 45 µrad |
| Antenna/receiver diameter | 1.8 m | 40 cm |
| Height coverage | 95 m to 20 km | 75 m to 35 km |
| Vertical resolution | 45 or 90 m | 7.5 m |
| Time resolution | 10 s | 0.5 s |
| Sensitivity | $\sim -40$ dBZ at 10 km | max OD $\sim 4$ |

Table 1: Technical characteristics of the MMCR and HSRL located near Eureka (respectively based on Moran et al., 1998, and Eloranta, 2005).

even though the intensity of the signal would not be affected by those. In fact, only its maximum observable height would be diminished, since a reference to the molecular channel is used to get the measurements. That method allows an absolute calibration of the measurements without any a priori assumptions about the attenuation due to the atmosphere or caused by things on the output window (Eloranta, 2005).

The two main HSRL measurements are the particulate backscatter cross section and the circular depolarization ratio. Recent work (Eloranta, 2005) suggests that, from those measurements, some microphysical characteristics can be retrieved, such as the particle effective size, the particle number density and the water content.

## 3 METHODOLOGY

Many characteristics of the clouds and surrounding air can be inferred from the synergetic measurements of the cloud radar and lidar. In clouds, lidar's backscatter $\beta$ ($sr^{-1}m^{-1}$) is proportional to the square of the diameter ($D$) of the hydrometeors ($\sim D^2$). Depolarization of lidar backscatter indicates that the scattering particles are non-spherical. This property provides a useful mean to discriminate between ice particles (non-spherical) and water droplets (spherical) in clouds. In typical mixed-phase conditions, liquid occurs as a high concentration of small spherical droplets, while ice is distributed in relatively low concentrations of large, non-spherical ice crystals. As a result, the lidar backscatter and depolarization ($\sim D^2$) signals are dominated by the high concentration liquid droplets, and areas with high intensity lidar backscatter and near-zero lidar depolarization signals indicate the presence of small liquid droplets.

The radar backscatter is proportional to the sixth power of the hydrometeor diameter ($\sigma \sim D^6$). Thus in typical mixed-phase conditions, the low concentration large ice crystals dominate the radar backscatter signal and MMCR observations offer little information about the spatial distribution of liquid in the atmospheric column. Furthermore, high radar reflectivity values can not be supported by small cloud droplets only and larger size particles are required (e.g., drizzle or large ice crystals). At subzero temperatures, drizzle growth is not favored. Thus, high MMCR reflectivities in clouds at subzero temperatures indicate the presence of ice crystals.

Our objective is to determine the number of layers, the hydrometeor (cloud and precipitation) fraction, the cloud types and the hydrometeor phases. The following discussion defines and explains each of these. To facilitate the comprehension, the results obtained for a single case (September 9, 2005) are also included (see Figs. 6 to 10), as an example. In fact, the methodology was applied to a variety of cloud and precipitation conditions (single- and multi-layer systems, with or without liquid hydrometeors...) before we apply it to the longer time period (15 months) available.

The MMCR and HSRL measurements taken on September 9, 2005 are reproduced in Figs. 3 and 4, respectively, and demonstrate the complexity of the situation. Up to 16 UTC, the returned HSRL signal shows the distinct signature of cloud droplets presence most of the time, causing the lidar signal to attenuate significantly, to the extend that HSRL measurements were not available anymore. On the other hand, the radar echo layer that appeared after 18 UTC seems to be well documented by both sensors. Finally, the lidar seems to have picked up a lot of aerosol in the lowest levels, as seen by the low backscatter values associated to low depolarization ratios.

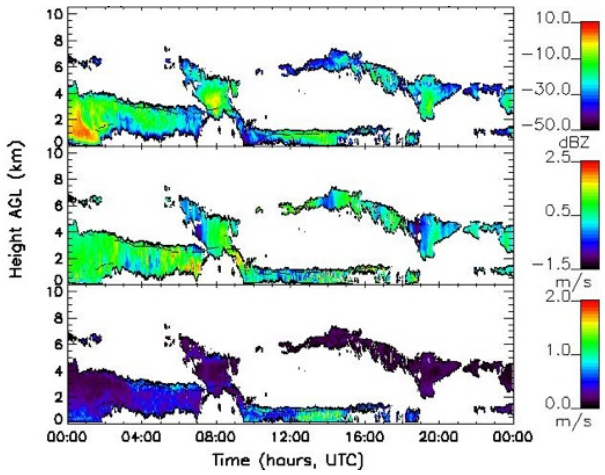


Figure 3: MMCR measurements from September 9, 2005. The upper panel shows the reflectivity factor, while the middle one represents the Doppler velocity and the lower, the spectral width. The black lines around the echoes are the radar echo boundaries, while the other black line, crossing the echoes, is the liquid cloud base, as defined by the lidar measurements.

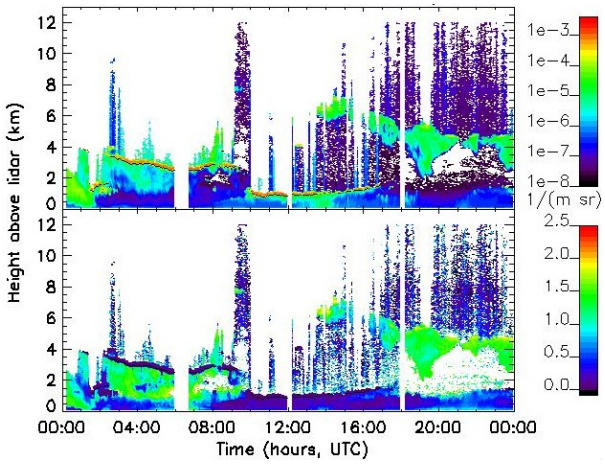


Figure 4: HSRL measurements from September 9, 2005. The upper panel shows the backscatter cross section, while the lower one represents the depolarization ratio. The black line in both panels marks the presence of cloud droplets seen by the lidar.

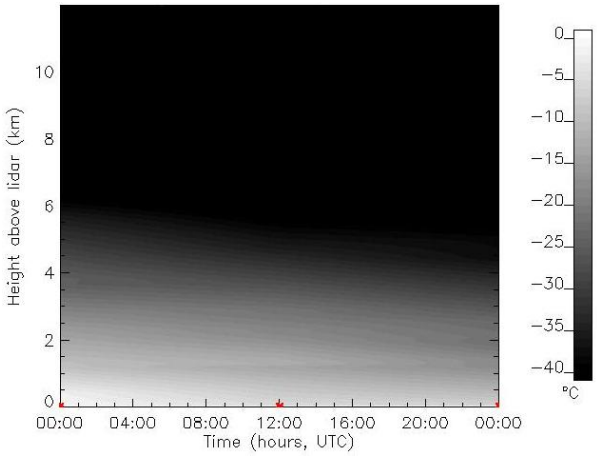


Figure 5: Temperatures of the atmosphere above Eureka on September 9, 2005, interpolated from three soundings taken at the time indicated by the red dots. Black regions have a temperature below $-40$ ℃, while white regions are at or above 0 ℃.

Three soundings are relevant for the analysis of that day. The adaptation of their resolutions to the lidar standards gives the temperatures shown in Fig. 5. It should be noticed that the atmosphere temperature never got above 0 ℃ according to this adaptation. However, it started so close to the freezing level at the surface, it is possible that it had exceeded it for a short period of time between the first soundings.

### 3.1 Cloud Occurrence and Cloud Layers

The number of cloud layers in an atmospheric column is rather easy to compute. But, first, a definition of a cloud layer is required. A *hydrometeor pixel* is defined to have an MMCR reflectivity factor above $-60$ dBZ. Of course, this is subjective to the instrument used for the cloud detection and its sensitivity. Using that, the *cloud layers* are simply groups of hydrometeor pixels encountered in the vertical atmospheric column. Each cloud layer starts (base) at the altitude of the first MMCR detection of a hydrometeor pixel (dBZ $> -60$) and ends (top) at the altitude the MMCR detects no hydrometeor pixel (dBZ $< -60$).

As shown in Fig. 6, hourly- and daily-averaged fractions (last column) of the occurrence of those hydrometeor pixels can be computed. The former represents well the atmospheric state. In fact, most radar echoes are still easily seen in them, with a varying intensity. It demonstrates that the presence

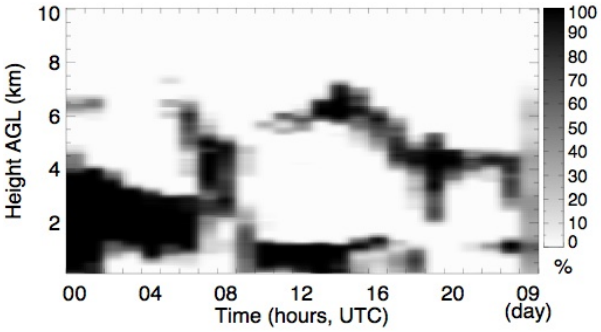


Figure 6: Hourly (first 24 columns) and daily (last column) hydrometeor fractions computed for September 9, 2005.

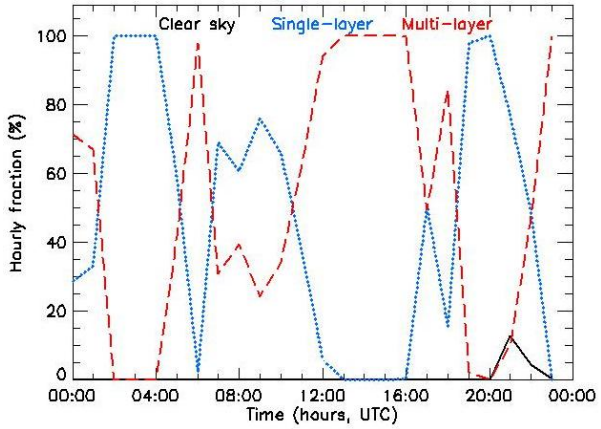


Figure 7: Hourly fraction of each cloud layer system observed on September 9, 2005: clear sky (continuous black line), single-layer (dotted blue line) and multi-layer (dotted red line).

of hydrometeors stay recognizable even after some averaging, especially if they are in deep layers and persist with time. In those situations, the fraction was greater than 80%.

Once the hydrometeor pixels are identified, three possible hourly-averaged cloud conditions are defined (base on MMCR measurements only): i) *clear sky*, when no cloud layer was observed in the whole column, ii) *single-layer*, when only one cloud layer was observed at that time and iii) *multi-layer*, when more than one cloud layer was observed in the column. A time-series of the occurrence of each can be computed, as shown in Fig. 7, in which a hourly-averaged occurrence is used. Besides the time period around 21 UTC, when clear conditions were observed for less than 15%, clouds were present in the sky, with multi-layer conditions occurring mostly between 12 and 18 UTC.

### 3.2 Cloud Type

Once the cloud layers are identified, we relate them with a particular cloud type based on their morphology (cloud base, top and thickness). Even though many types can be defined, only four of them are used in this project. The categories are i) *high* (cirrus) clouds, with a base higher than 5 km, ii) *middle* (alto) clouds, with a base higher than 2 km, but lower than 5 km, iii) *low* clouds, with base and top lower than 2 km, and iv) *deep* clouds, with a base lower than 2 km and a top higher than 2 km.

These cloud types evolve with time and they can change from one time to another. The cloud types are further divided into two categories each: containing precipitation (reaching or not the surface) and precipitation free. A scheme to differentiate the precipitation from the actual cloud is then required. This is quite easy for the liquid cases: if the reflectivity factor is higher than $-17$ dBZ, precipitation-size particles should be present in that echo layer and it is safe to say that layer is precipitating. The Doppler velocity can also help. If it is greater than 2.5 m/s, the signal is most likely made of falling liquid, as ice crystals fall at much lower speeds.

On the other hand, it is harder for the solid (and mixed-phase) cases, where a similar threshold value can not be defined as easily, as it would depend upon the shape of the crystals (among other factors). Nevertheless, in this project, its value is taken to be 0 dBZ for the solid cases, a very conservative one, while none is set for the mixed-phased cases and they are simply considered as clouds. These radar reflectivity threshold values are summarized in Fig. 8a, for all the possible hydrometeor phases considered in this project.

The HSRL provides a mean for a more complete echo classification into cloud and precipitation, using the liquid layers it found. Thus, within an MMCR echo layer, if there is a liquid base, every signal below it is said to precipitate, while everything above is set to cloud. However, if no HSRL measurement is available in the whole column, the type is set to unknown. Finally, if the lidar signal is clear inside a radar echo layer, it is said to be due to aerosols.

Fig. 9 shows the occurrence of each cloud type, after the radar echoes have been discriminated between cloud and other causes (precipitation or aerosols). It can be seen that the first layer started with a low base and precipitated to the ground. Then, its base got higher and its precipitation turned

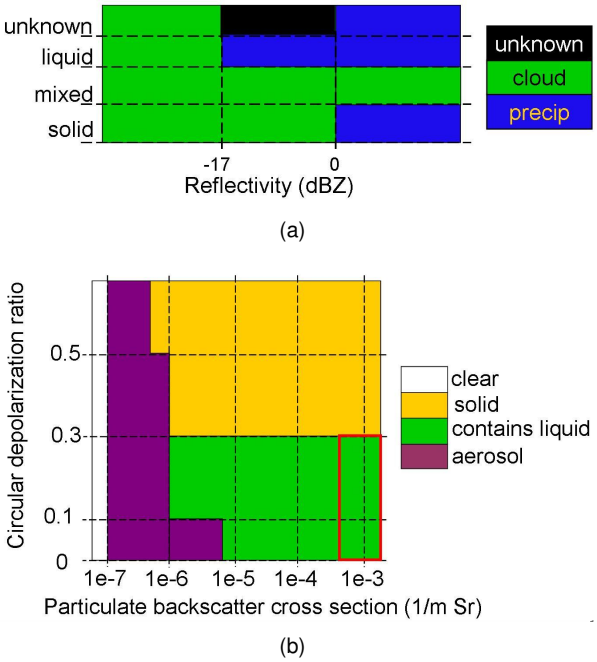


Figure 8: (a) MMCR reflectivity threshold values used for the echo classification, depending on its phase. (b) HSRL classification using both of its measurements. The red box indicates the criteria to find cloud droplets.

into virga (evaporating/sublimating before reaching the ground). And, finally, it merged with a higher cloud. The stratiform boundary layer cloud detected in the middle of the day was rather shallow and precipitation originating at its lidar-defined base reached the ground only around 12 UTC, while its height and depth stayed rather constant the whole time it was observed. The high cloud observed after 12 UTC grew in depth rapidly, while its base stayed constant, thus keeping its type classification. However, its base then dropped, while its depth stayed constant, eventually turning it into a middle cloud.

A few aerosols are seen in Fig. 9. However, the lidar detected more of them in the boundary layer, as will be seen in the next section.

### 3.3 Hydrometeor Phase

The hydrometeor phase is a more difficult cloud parameter to retrieve. As discussed before, the HSRL measurements provide a first mean of classification. High lidar backscatter and low circular depolarization ratio are good indicators of the presence of cloud droplets in the observed volume. On the contrary, if the lidar backscatter is low (below a sub-

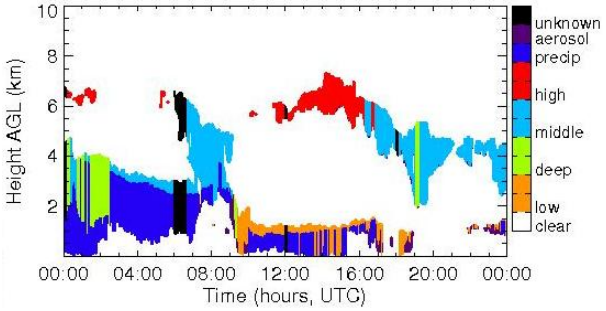


Figure 9: Types of cloud observed on September 9, 2005.

jective threshold), the particles hit by the HSRL are not numerous enough to be considered hydrometeors: they are most probably aerosol. Furthermore, some regions return so little power that they can be declared clear. Finally, it is quite rare that the HSRL sees a liquid drop as non-spherical, since it is sensing its horizontal cross section only. Thus, as the depolarization ratio gets bigger, the possibilities to find liquid diminishes and, at some point, the signal is said to be due to solid particles only.

Those conclusions are summarized in the chart given in Fig. 8b, which includes the threshold values used in this project. Thus, the HSRL provides a first estimate of the location of the hydrometeors in the profiles, as well as their phase.

A first refinement is obtained using the temperature profiles. For instance, wherever the temperature gets below $-40$°C, the hydrometeors must be solid: homogeneous nucleation of ice occurs then. At the opposite, a temperature above 0°C indicates liquid hydrometeors: ice should melt there. Between those limits, the Doppler velocity can help: if it is greater than 2.5 m/s downwards, the signal is most likely made of liquid precipitation.

Finally, some general rules are added. If the HSRL signal gets attenuated by crystals only before the end of an MMCR echo layer, the phase found at the last good HSRL signal is kept up to the top of that layer, while the layers above it have unknown phase. However, if the HSRL signal gets attenuated by numerous cloud droplets, the phase of every MMCR echo above is unknown. Obviously, the temperature criteria still hold.

The results of this phase classification is shown, with the results of the echo classification, in Fig. 10. As mentioned before, the lidar detected a lot of aerosols in the boundary layer, as can be seen in Fig. 10a. Most of the unknown phases observed in Fig. 10b are caused by the missing data in the lidar returned signal, either due to a strong attenuation

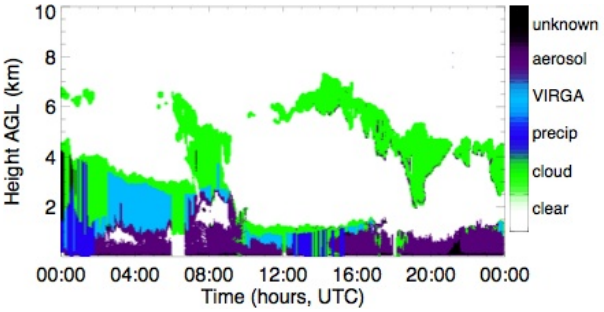


(a)

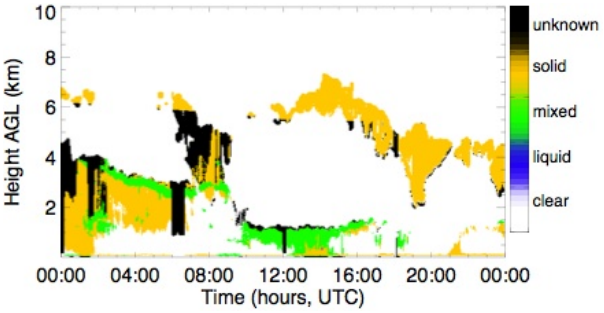


(b)

Figure 10: Results of the echo (a) and phase (b) classifications for September 9, 2005.

by numerous cloud droplets or a non-functioning lidar. Also, the sharp boundary near 6 km, where every signal is put to solid, is due to the temperature being below $-40$°C above that height.

Looking at the two panels of Fig. 10, it can be observed that all high clouds are formed of ice only. Also, everything precipitating from the deep cloud (the first one) is completely frozen as soon as it leaves the liquid base. On the opposite, the thin boundary layer cloud (around 12 UTC) seems to have kept is precipitation into a mixed of phases until it almost reached the ground.

Data from both instruments have been processed for about 15 months. A cloud occurrence, type and phase climatology will be computed as part of our future research work.

## 4 ACKNOWLEDGEMENTS

This work is being funded by the Natural Sciences and Engineering Research Council of Canada (NSERC) Graduate Scholarship program. The MMCR and HSRL data has been provided by Matthew D. Shupe and Edwin W. Eloranta, respectively.

## 5 REFERENCES

Ackerman, T. P. and G. Stokes, 2003: The Atmospheric Radiation Measurement program, *Phys. Today*, **56**, 38-45.

Clothiaux, E. E., T. P. Ackerman, G. G. Mace, K. P. Moran, R. T. Marchand, M. A. Miller and B. E. Martner, 2000: Objective determination of cloud heights and radar reflectivities using a combination of active remote sensors at the ARM CART sites, *J. Appl. Meteor.*, **39**, 645-665.

Eloranta, E. W., 2005: High spectral resolution lidar, in 'Lidar: Range-Resolved Optical', K. Weitkamp, ed. Springer-Verlang, New York.

Gregory, D. and D. Morris, 1996: The sensitivity of climate simulations to the specification of mixed phase clouds, *Climate Dyn.*, **12**, 641-651.

Moran, K. P., B. E. Martner, M. J. Post, R. A. Kropfli, D. C. Welsh and K. B. Widener, 1998: An unattended cloud-profiling radar for use in climate research, *Bull. Amer. Meteor. Soc.*, **79**(3), 443-455.

Shupe, M. D., 2007: A ground-based multiple remote-sensor cloud phase classifier, *Geophys. Res. Lett.*, in press.

Shupe, M. D., S. Y. Matrosov and T. Uttal, 2006: Arctic mixed-phase cloud properties derived from surface-based sensors at SHEBA, *J. Atmos. Sci.*, **63**, 697-711.